5-1-2000

Turbidite Megabeds in an Oceanic Rift Valley Recording Jokulhlaups of Late Pleistocene Glacial Lakes of the Western United States

G.G. Zuffa
Universitá di Bologna

W.R. Normark
Universitá di Bologna

F. Serra
University of Southern Mississippi

Charlotte A. Brunner
University of Southern Mississippi, charlotte.brunner@usm.edu

ARTICLES

Turbidite Megabeds in an Oceanic Rift Valley Recording Jökulhlaups of Late Pleistocene Glacial Lakes of the Western United States

G. G. Zuffa, W. R. Normark,[1] *F. Serra, and C. A. Brunner*[2]

Dipartimento di Scienze della Terra e Geologico-Ambientali, Università di Bologna, Via Zamboni 67, 40127 Bologna, Italy
(e-mail: zuffa@geomin.unibo.it)

ABSTRACT

Escanaba Trough is the southernmost segment of the Gorda Ridge and is filled by sandy turbidites locally exceeding 500 m in thickness. New results from Ocean Drilling Program (ODP) Sites 1037 and 1038 that include accelerator mass spectrometry (AMS) ^{14}C dates and revised petrographic evaluation of the sediment provenance, combined with high-resolution seismic-reflection profiles, provide a lithostratigraphic framework for the turbidite deposits. Three fining-upward units of sandy turbidites from the upper 365 m at ODP Site 1037 can be correlated with sediment recovered at ODP Site 1038 and Deep Sea Drilling Program (DSDP) Site 35. Six AMS ^{14}C ages in the upper 317 m of the sequence at Site 1037 indicate that average deposition rates exceeded 10 m/k.yr. between 32 and 11 ka, with nearly instantaneous deposition of one ~60-m interval of sand. Petrography of the sand beds is consistent with a Columbia River source for the entire sedimentary sequence in Escanaba Trough. High-resolution acoustic stratigraphy shows that the turbidites in the upper 60 m at Site 1037 provide a characteristic sequence of key reflectors that occurs across the floor of the entire Escanaba Trough. Recent mapping of turbidite systems in the northeast Pacific Ocean suggests that the turbidity currents reached the Escanaba Trough along an 1100-km-long pathway from the Columbia River to the west flank of the Gorda Ridge. The age of the upper fining-upward unit of sandy turbidites appears to correspond to the latest Wisconsinan outburst of glacial Lake Missoula. Many of the outbursts, or jökulhlaups, from the glacial lakes probably continued flowing as hyperpycnally generated turbidity currents on entering the sea at the mouth of the Columbia River.

Introduction

The Gorda Ridge, which lies offshore northern California and southern Oregon between the Blanco and Mendocino Fracture Zones (fig. 1), is the only oceanic spreading center that lies entirely within the Exclusive Economic Zone (EEZ) of the United States. The Gorda Ridge changes from a medium-rate (5.8 cm/yr) spreading ridge at its northern terminus with the Blanco Fracture Zone to a slow-rate (~2 cm/yr) spreading ridge near the Mendocino Fracture Zone in the south, where the axial rift valley is bounded by mountainous ridges as high as 2 km. The southernmost segment of the Gorda Ridge (south of lat 41°00′) has a deep axial rift valley, the Escanaba Trough, which widens to the south, and the relief of the flanking ridges decreases abruptly and disappears before intersecting the Mendocino Fracture Zone (fig. 1). The Escanaba Trough is floored by sediment over most of its length (Moore and Sharman 1970), and thick sections of sediment fill occur along the base of the Mendocino Fracture Zone on both flanks of the Gorda Ridge. A sill slightly shallower than 3100 m water depth at the north end of the Escanaba Trough marks the northern limit of the sediment fill (fig. 1).

Sampling the sediment fill of the Escanaba Trough was one of the earliest objectives of the Deep Sea Drilling Program (DSDP). Drilling at DSDP Site 35 sampled selected intervals, attempting to core only about 145 m of the sediment fill

Manuscript received July 23, 1999; accepted January 6, 2000.
[1] U.S. Geological Survey, MS 999, 345 Middlefield Road, Menlo Park, California 94025, U.S.A.
[2] Department of Marine Science, University of Southern Mississippi, Stennis Space Center, Mississippi 39529, U.S.A.

[The Journal of Geology, 2000, volume 108, p. 253–274] © 2000 by The University of Chicago. All rights reserved. 0022-1376/2000/10803-0001$01.00

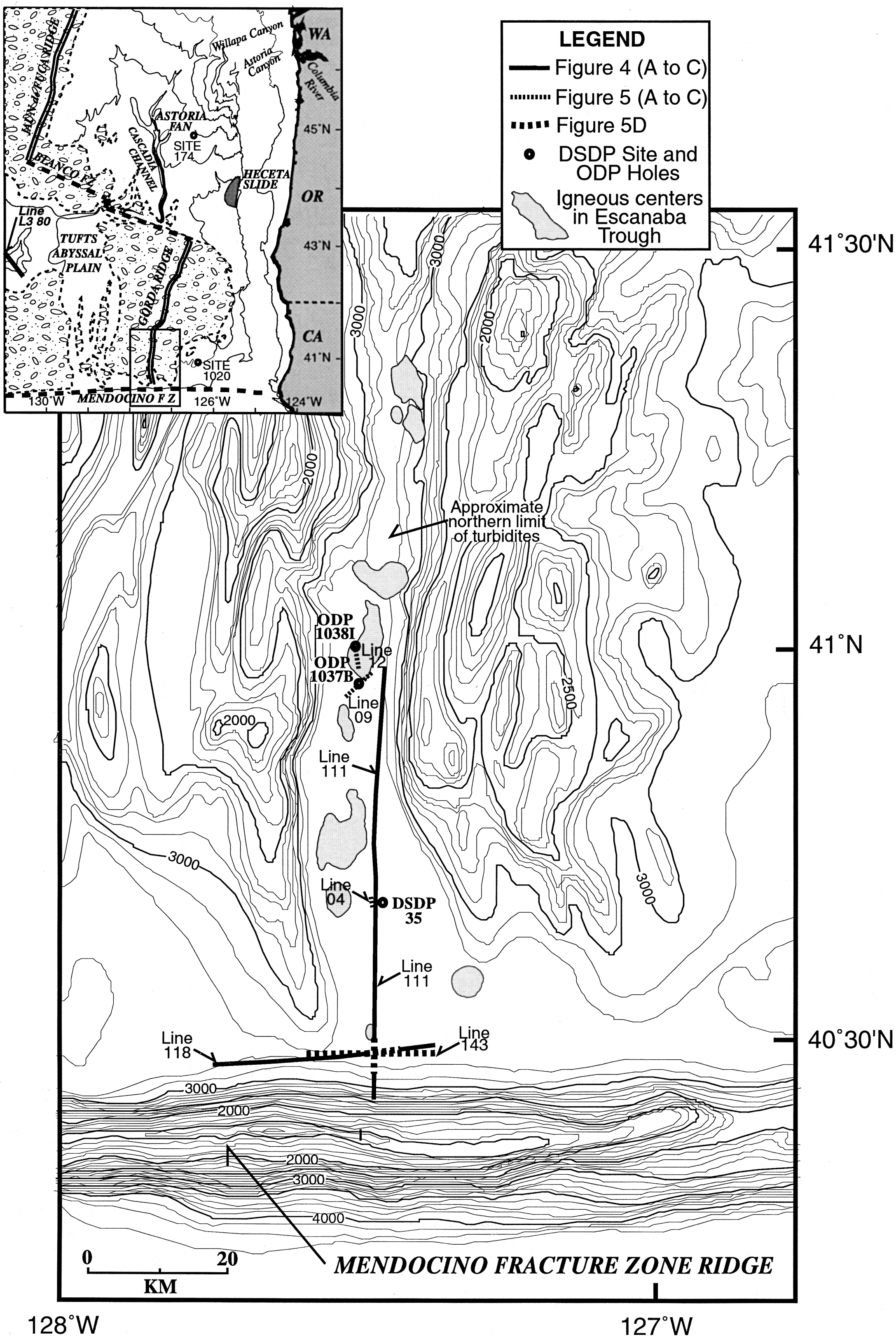

Figure 1. Bathymetric map of Escanaba Trough, adapted from Smith and Sandwell (1997), showing igneous centers, DSDP Site 35, ODP Sites 1037 and 1038 (modified from Shipboard Scientific Party 1998*c*), and location of seismic-reflection profiles in figures 4*A*, 4*B*, and 5*A*–5*D*. Inset shows location and setting of Escanaba Trough (rectangular box at southern end of Gorda Ridge) and location of line L3 80 shown in figure 4*C*.

to a hole depth of 390 m (fig. 2; Moore and Sharman 1970; Shipboard Scientific Party 1970). Much of the recovered sequence is turbidite deposits, and the petrography of the sandy beds suggested that turbidites in the upper part of the sediment fill come from the distant Columbia River, whereas those near the bottom of the hole might be from the much nearer Klamath River (Vallier et al. 1973; Zuffa et al. 1997). This early DSDP sampling provided no information on the age of the turbidite fill, which was unlikely to be older than latest Pleistocene (<100 ka) because of the active rifting and creation of new oceanic crust along the ridge axis (see discussion in Normark et al. 1994).

As a result of an effort by the U.S. Minerals Management Service to lease the entire Gorda Ridge area for mineral exploitation following the declaration of the U.S. EEZ, the Escanaba Trough became the focus for detailed geological and geophysical survey efforts (see extensive reviews in McMurray 1987; Morton et al. 1994*b*). Volcanogenic massive sulfide deposits and associated hydrothermal vents were found at several localities on and within the sediment fill near the axis of the Escanaba Trough (Koski et al. 1994; Morton et al. 1994*a*; Zierenberg et al. 1994). To understand the interaction of the hydrothermal fluids with the host sedimentary sequence, the lateral extent, sedimentologic processes, and thermal structure of the axial valley fill were investigated (e.g., Davis and Becker 1994; Morton and Fox 1994; Normark et al. 1994). The areas of volcanogenic massive sulfides are generally associated with hills formed by local uplifts of the turbidite fill. The lateral connectivity of the turbidite sand units provides pathways for the hydrothermal fluids to migrate horizontally within the sediment. Migration of hydrothermal fluids could explain the diagenetic effects on the sediment suggested by the petrography of samples recovered at DSDP Site 35 (Vallier et al. 1973; Zuffa et al. 1997). The most northerly site of hydrothermal mineralization in the Escanaba Trough was subsequently chosen for Ocean Drilling Program (ODP) drilling (Fouquet et al. 1998).

Most of the sand-sized material recovered from the turbidite fill of the Escanaba Trough at DSDP Site 35 is clearly from the North American continent (Vallier et al. 1973; Zuffa et al. 1997); the pathway followed, especially considering the inferred source from the Columbia River drainage basin, is less certain. The continental margin of the western United States north of the Mendocino Fracture Zone is an accretionary prism that incorporates turbidites and pelagic sediment deposited on a series of submarine fan systems that extend from the Nitinat fan north of the Columbia River to the Eel fan at the base of the Mendocino Fracture Zone (fig. 1; Carlson and Nelson 1987; Clarke 1987; Snavely 1987). North of the Blanco Fracture Zone, the modern turbidite fans have buried much of the subducting plate and the easternmost part of the fracture zone as well. The turbidite fan systems off northern California are much less extensive and only locally bury the ridge topography of the eastern flank of the Gorda Ridge. A large mass failure deposit, the Heceta submarine slide (fig. 1, inset), at 44°N latitude on the Oregon continental margin, has blocked turbidity currents initiated off the Columbia River from reaching the area south of the Blanco Fracture Zone along the base of the continental slope since the time of the failure about 110 ka (Goldfinger et al. 2000). Before 110 ka, a turbidite channel from Astoria Canyon extended across the fracture zone to the eastern flank of Escanaba Trough.

Another possible route for Columbia River sediment to reach the Escanaba Trough is from the west, across the Pacific flank of the Gorda Ridge. Hurley (1960, 1964) described the Cascadia Channel, which extends offshore from the Columbia River south into and through the Blanco Fracture Zone; the channel exits from the fracture zone onto the Pacific plate and extends west for several hundred kilometers on the Tufts Abyssal Plain. Griggs et al. (1970) described pebble-sized sediment from the floor of Cascadia Channel west of the Blanco Fracture Zone that they ascribed to an eastern Washington source area; they further suggested that this coarse material was carried to the ocean by the late Pleistocene catastrophic floods from glacial Lake Missoula and subsequently transported through Cascadia Channel to the Pacific plate.

The purpose of this article, which expands considerably the preliminary results, first reported by Brunner et al. (1999), is to reevaluate the source area, transport paths, and depositional processes that provided the turbidite fill within the Escanaba Trough. Our study is based on: (1) new petrographic data from sand-sized sediment recovered during ODP Leg 169 at Sites 1037 and 1038; (2) stratigraphic control provided by deep-tow, high-resolution 4.5-kHz seismic-reflection profiles obtained as part of a site-survey activity for Leg 169; (3) ages of the turbidite deposits based on accelerator mass spectrometry (AMS) ^{14}C data from reference Hole 1037B and Hole 1038I; and (4) interpretation of new seismic-reflection data to evaluate the stratigraphic relation between the turbidite fill in the Escanaba Trough and the sediment deposited on both flanks of the Gorda Ridge. These new data

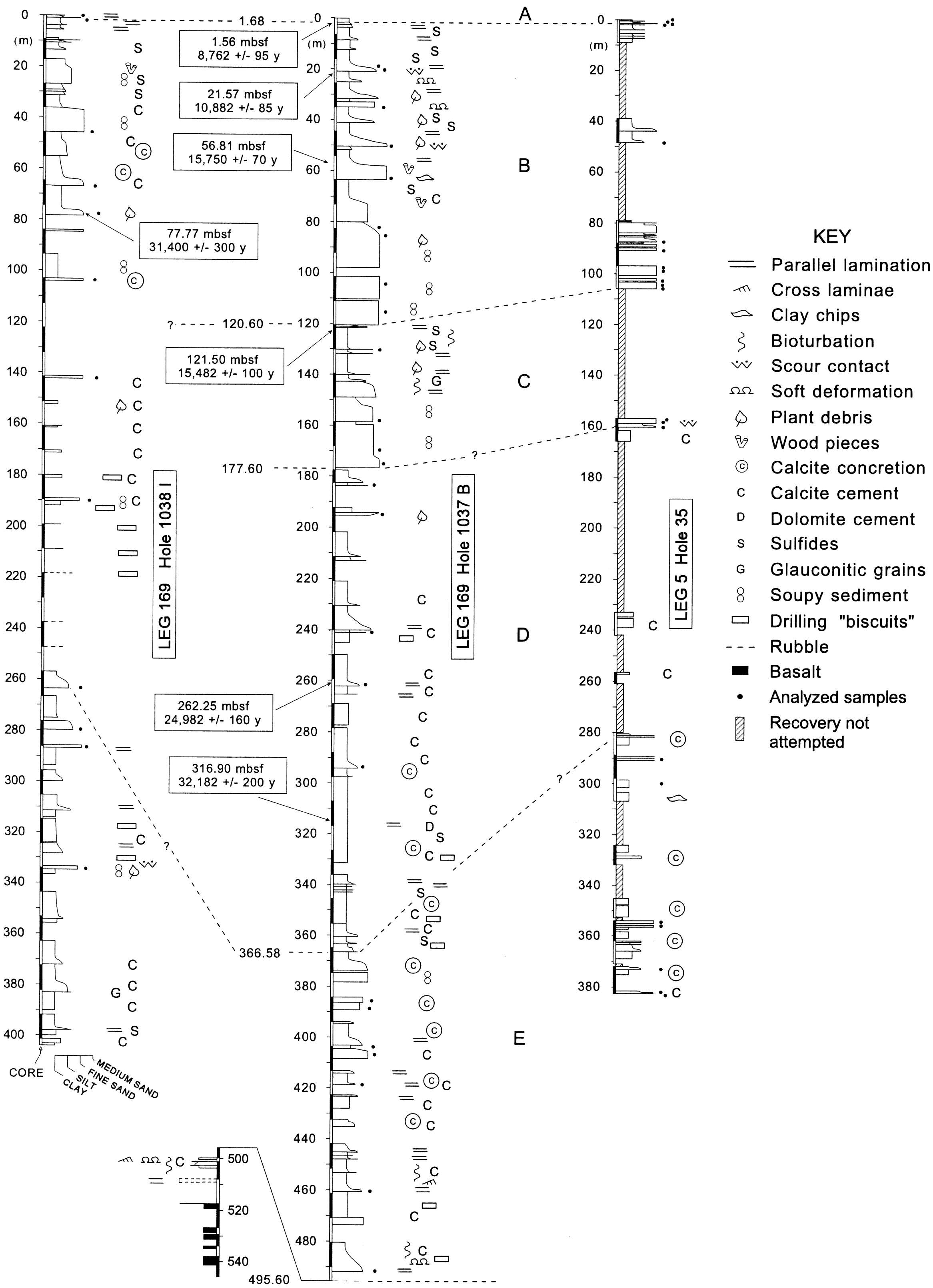

Figure 2. Graphic sedimentation columns for Holes 1038I and 1037B and DSDP Site 35 (see also Shipboard Scientific Party 1970, 1998*a*, 1998*b*). Uppercase letters denote lithostratigraphic units defined in this article for Hole 1037B; dashed lines show probable correlation of these units with Site 35 and Hole 1038I.

allow a direct correlation with the previous samples recovered at the more southerly DSDP Site 35 and show that the results based on the Leg 169 drilling can be applied to the turbidite fill along the entire 75-km length of the Escanaba Trough. The volume and age of the upper part of the turbidite deposits indicate that they accumulated in a very short time interval (≤5 k.yr.) and suggest that the deposits might have been generated as a result of outbursts from glacial lakes of the Pacific northwest.

Lithostratigraphy

Site 1037. The core stratigraphy at reference Hole 1037B (fig. 2) was constructed on the basis of visual core descriptions made onboard Leg 169. Eight lithostratigraphic units were distinguished on the ship, chiefly on the basis of sand/silt-dominant versus mud-dominant turbidites and sedimentary structures, but also using magnetic susceptibility data that, with few exceptions, distinguished the graded turbidite layers (Shipboard Scientific Party 1998*b*). A nearly complete sedimentary sequence (495.60 m) was recovered. A rubble comprising metamorphosed claystone and siltstone was recovered beneath the turbidite sequence between 495.60 and 507.80 mbsf (meters below sea floor). The base of the cored interval consists of basalt that was recovered from 507.80 to 546 mbsf.

The lithostratigraphic units of the Shipboard Scientific Party (1998*b*) are reinterpreted in this report and are based on stratigraphic trends, depositional-process similarities, and sediment age in addition to the lithology, which was the primary basis for distinguishing units during Leg 169. The description of the revised lithostratigraphic units follows.

Unit A (Holocene). This unit consists mostly of hemipelagic, fossiliferous, unconsolidated greenish-gray clay and extends downcore to 1.68 mbsf, which corresponds to the top of the first turbidite bed of the underlying unit B. The AMS ^{14}C dating of planktonic foraminifers at 1.56 mbsf gave an age of 8762 ± 95 yr (table 1; fig. 2). The implied Holocene sedimentation rate is in agreement with previous determinations from Escanaba Trough (Karlin and Lyle 1986).

Unit B (Late Pleistocene). Unit B consists of a fining- and thinning-upward sequence of megaturbidite beds that extends to 120.60 mbsf. It contains a basal package (from 120.60 to 63.52 mbsf) of massive, dark gray, fine- to medium-grained sand grading upward to pelite in the upper 6 m. Small pieces of woody material are present throughout this stratigraphic interval. The basal sand megabed is overlain by a sequence of 10 thinning-upward, well-defined megaturbidite beds (from 63.52 to 1.68 mbsf). This sequence shows a distinct fining upward from fine- to very fine-grained sand to silt and clay. A thin hemipelagite layer near the top of the unit at 21.57 mbsf is 10,882 ± 85 yr old, and a pinecone scale near the base of the unit at 56.81 mbsf is 15,750 ± 70 yr old, based on AMS ^{14}C dating.

Unit C (Late Pleistocene). This unit is lithologically similar to unit B. It consists of a fining- and thinning-upward sequence that extends from 177.60 to 120.60 mbsf. The basal 35 m of this unit consist of massive, dark gray, very fine- to medium-grained, very poorly sorted sand that is interpreted to consist of three megaturbidite beds (fig. 2). The unit fines upward and in the upper part includes six mud turbidite beds with thin basal intervals of finely laminated, dark gray, fine sand and silt that fines upward to silty clay and clay. A hemipelagic layer at the top of the unit is 15,482 ± 100 yr old based on AMS ^{14}C dating.

Unit D (Late Pleistocene). This unit extends downhole to 366.58 mbsf and consists of thick turbidite beds fining upward from thin intervals of silt or very fine-grained sand to clay. The AMS ^{14}C dating of planktonic foraminifers at 262.25 and 316.90 mbsf gave ages of 24,982 ± 160 yr and 32,182 ± 200 yr, respectively.

Unit E (Late Pleistocene). This unit extends to 495.60 mbsf and consists dominantly of dark gray siltstone and minor fine-grained moderately indurated sandstone turbidite beds of variable thickness. A greater number of beds occurs in this unit than in overlying units, and parallel-, wavy-, and cross-lamination are more common structures here than in the overlying unit D.

Site 1038. On the basis of core lithology (fig. 2), the upper 78 m of Hole 1038I can be correlated reasonably well with reference Hole 1037B. Poor recovery between 100 and 258 mbsf prevents reliable correlation in the middle part of the section at Hole 1038I. The lower part of the section at Hole 1038I (from 258 to 403 mbsf) cannot be correlated bed by bed with reference Hole 1037B, but the lithology, the structures, and the style of the turbidite beds appear similar to unit E.

Site 35. On DSDP Leg 5, drilling at Site 35 extended to nearly 400 mbsf in the southern part of Escanaba Trough, but the section was not continuously cored. Poor recovery and discontinuous coring resulted in sampling of only about 25% of the total hole depth. Although recovery was notably poor in the interval from 106 to 280 mbsf, a 25-m-thick sand interval between 80 and 105 mbsf was

Table 1. Accelerator Mass Spectrometry ^{14}C Dates Used to Estimate Sedimentation Rates

Site, core, and section sampled (cm)	Depth (mbsf)	Age (yr)	Error (+/−yr)	Ocean reservoir correction (yr)	Corrected age (yr)	AMS laboratory sample number	Lithologic unit	Host lithology and depth to calculate sedimentation rate	Material dated
1037B-1H-2 (6-8)	1.56	9480	95	−718	8762	NOSAMS OS-12352	A	H, base at 1.68 mbsf, ~9436 ka	Pf
1037B-3H-4 (97-100)	21.57	11,600	85	−718	10,882	NOSAMS OS-12620	B	H at top of a turbidite	Pf
1037B-7H-2 (121-124)	56.81	15,750	70	...	15,750	NOSAMS OS-11810	B	T, base at 63.6 mbsf	Pcs
1037B-7H-3 (124-128)	58.10	35,800	370	...	35,800	NOSAMS OS-11811	B	T, base at 63.6 mbsf	Wa
1037B-8H-CC (26-28); 1037B-9H-1 (0-4)	73.10	20,230	160	...	20,230	ETH-17054/6	B	T, base at 82.47 mbsf	C
1037B-8H-CC (26-28)	73.07	43,510	1190	...	43,510	ETH-17055	B	T, base at 82.47 mbsf	Wb
1037B-9H-1 (0-4)	73.12	33,590	470	...	33,590	ETH-17057	B	T, base at 82.47 mbsf	Wb
1037B-14H-1 (89-92)	121.50	16,200	100	−718	15,482	NOSAMS OS-13927	C	H at top of a turbidite	Pf
1037B-29X-2 (135-137)	262.25	25,700	160	−718	24,982	NOSAMS OS-14127	D	H at top of a turbidite	Pf
1037B-34X-CC (29-31)	316.90	32,900	200	−718	32,182	NOSAMS OS-13928	D	H	Pf
1038I-9X-3 (37-39)	77.77	31,400	300	...	...	NOSAMS OS-11812	B	T, base 84-100 mbsf	Wb

Note. Pf, planktonic foraminifers; Pcs, pinecone scale (1.5 × 2.0 × 0.4 cm); Wa, wood (5.0 × 0.8 × 0.5 cm); Wb, wood (<mm-sized pieces); C, charcoal; H, Hemipelagite; T, Turbidite. For lithologic units see figure 2.

correlated with the massive sand interval of unit B (fig. 2). Sand intervals recovered from ~160 mbsf might correspond to the thick basal sand interval of unit C. Discontinuous and incompletely recovered sandy turbidite beds are also present in the basal portion of the section between 280 and 382 mbsf and might correlate with unit E in the reference hole.

Geochronology

Methods. More than 200 samples from Hole 1037B were examined for carbon-rich materials suitable for ^{14}C dating by AMS. Five samples containing wood and charcoal were extracted from wood-bearing intervals observed during physical description of the cores (table 1). The remaining samples were taken from the topmost clay-and-silt units of turbidites in hopes of sampling planktonic foraminifers from hemipelagites, which best indicate the emplacement age of the underlying turbidite. Most of the samples, however, were barren of foraminifers or contained less than the minimum 10 mg of carbonate material that is required for AMS ^{14}C dating.

Samples that contained enough planktonic foraminifers for AMS ^{14}C dating were evaluated further to determine whether the samples were hemipelagic or turbiditic. A census of the benthic foraminifers was used to reject those samples with more than ~20% neritic and upper bathyal taxa in the >150-μm fraction. The neritic and upper bathyal constituents indicate that the samples might be turbiditic or might contain admixtures of resedimented material. Five samples of planktonic foraminifers were accepted for AMS ^{14}C dating.

Foraminifer tests were cleansed of detrital matter by sonification in a hot 1% solution of Calgon. The tests were subsequently rinsed in distilled water, dried, and bottled in clean glass vials. Wood was rinsed in a dilute (10%) HCl solution to remove adhering carbonate, then rinsed in distilled water and bottled in clean glass bottles for shipment.

The AMS ^{14}C analyses were done by the National Ocean Sciences Accelerator Mass Spectrometry Facility (NOSAMS). Ages were reported using a radiocarbon half-life of 5568 yr. Ages of planktonic foraminifer samples were corrected for a regional ocean reservoir effect of −718 yr (Southon et al. 1990). Ages were not corrected to calendar years, so they are more comparable to ages reported from the Washington Scabland (Waitt 1985; Atwater, 1986).

Sedimentation rates in the turbidite sequence at Hole 1037B were calculated using two sets of criteria, one for turbidites and one for hemipelagites. Turbidites are deposited over a geologically short time interval, perhaps days or weeks, and can be viewed as essentially instantaneous events. Turbidites comingle older reworked sediment with contemporaneous material. Therefore, interpretation of dates on samples from turbidites must take into account both effects in order to estimate sedimentation rates. In cases where more than one sample was dated from a single turbidite, the youngest age was considered the best estimate of the age of turbidite emplacement. The appropriate depth to assign a date from a turbidite is the base of the bed because emplacement of the turbidite is essentially instantaneous. In the case of hemipelagites, however, no adjustment for the depth of the dated hemipelagic sample is needed in order to calculate the sedimentation rate.

Age and Sedimentation Rates. Six dates were selected for use: five dates on planktonic foraminifers from hemipelagic layers and one date on a large pinecone scale from a turbidite (table 1; fig. 3*A*). The age of the latter is viewed with some caution as a maximum possible age because the scale is reworked and could be older than the age of emplacement of the turbidite. All other dates were rejected on the basis of the selection criteria discussed above. Specifically, the dates were made on pieces of reworked charcoal and wood from turbidites, and the ages were substantially older than other materials dated from within the turbidites or from hemipelagic units below turbidites. Dates range from the early Holocene at 8762 ± 95 yr to oxygen isotope stage 3 at 32,182 ± 200 yr.

A sedimentation rate curve was plotted using the six selected dates. Average sedimentation rates exceeded 10 m/k.yr. below unit A, which is the hemipelagite that caps the sequence (fig. 3*A*). The upper part of unit B was deposited at rates averaging 13.8 and 8.6 m/k.yr., and the lower part of unit B, which is a >50-m-thick sand bed, was deposited essentially instantaneously. Unit C and the upper part of unit D were deposited at 14.8 m/k.yr., and the lower part of unit D was deposited at 7.6 m/k.yr. Measured sedimentation rates are comparable to previously estimated rates (Normark et al. 1994; Davis and Becker 1994) and confirm extraordinarily fast deposition at Escanaba Trough.

Acoustic Stratigraphy

Air-Gun Seismic-Reflection Profiles. The sediment fill within the axis of the Escanaba Trough extends more or less continuously at least 75 km northward from the north flank of the Mendocino Fracture

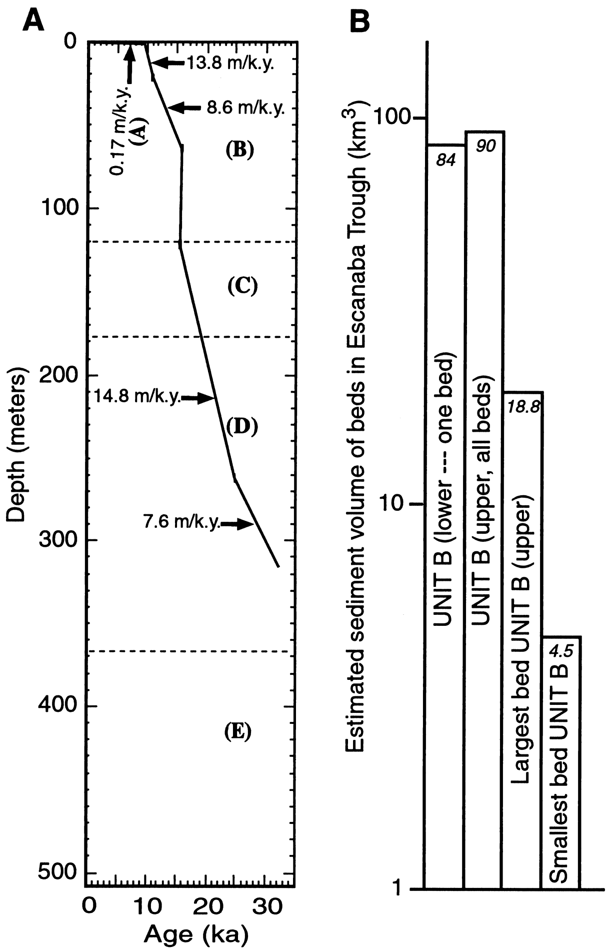

Figure 3. *A*, Sedimentation rate curve for Hole 1037B based on accelerator mass spectrometry ^{14}C ages of turbiditic and hemipelagic intervals (table 1). *B*, Estimated volumes of the Missoula-flood-source turbidites in Escanaba Trough.

Zone (fig. 4*A*). The sediment fill locally exceeds 500 m in thickness, and the sea floor is offset along faults that maintain the axial graben of the Gorda Ridge. Offset of the sea floor mimics that of the subbottom reflectors, suggesting that either displacement occurred after the sediment fill was emplaced or sedimentation was relatively uniform across the axial graben despite the sea floor offsets. In general, the upper 200 m of sediment along the axis appears uniform in reflection character compared with the deeper intervals (fig. 4*A*) except where there is possible volcanic intrusion, for example, 7 km north of DSDP Site 35.

The high relief of the ridges that bound the Escanaba Trough decreases abruptly to the south, and the southern ends of the ridge flanks, north of the Mendocino Fracture Zone, are buried by sediment (fig. 1). An east-west profile across the mouth of the Escanaba Trough (fig. 4*B*) clearly shows the down-dropped axis of the Trough with >600 m of sediment fill. The thick sediment fill wedges out <20 km east of the axis. In contrast, thick sediment fill characterizes the interridge valleys on the west flank of Gorda Ridge. The extensive sediment section along the north flank of the Mendocino Fracture Zone extends 150 km west (near 129°25′W; fig. 1).

Deep-Tow 4.5-kHz High-Resolution Profiles. A detailed site survey to obtain deep-tow side-looking sonar images and 4.5-kHz seismic-reflection profiles of the northern Escanaba Trough was conducted several months before Leg 169 (Ross et al. 1996). The grid of high-resolution 4.5-kHz profiles, with a line spacing of 1–2 km in the area of Sites 1037 and 1038, defines a distinct stratigraphic sequence of key reflectors in the upper 70 m of sediment that could be observed throughout the area. The "type locality" of the key reflectors is from line ET 09 at the location of Site 1037 (figs. 5*A*, 6). Eight key reflectors, denoted from the top down as B–I, are found on the valley floor and lower bounding terraces within the Escanaba Trough over a depth range of >150 m of relief on the trough floor (fig. 5). Figure 6 shows that the key reflectors correspond to the bases of the thinner, shallower turbidites and to the tops of the turbidites with thicker sand intervals. The physical properties recorded in the shipboard core logs mimic the graded bedding of the turbidites. Three additional, weak, and discontinuous reflectors observed at the type locality (Site 1037) include the shallowest (reflector A), a reflector that is generally found above D (about a third of the spacing between C and D), and a reflector just above F. These three reflectors were not recognized over the entire survey area and were not included as part of the key reflector sequence. The greatest variability in reflector character is in the interval between the sea floor and reflector B, where from none to as many as three reflecting surfaces were observed locally. Previous studies have shown that the upper 2 m of sediment in Escanaba Trough include thin, locally initiated turbidites that are not laterally extensive (Karlin and Lyle 1986; Normark et al. 1994). The variable number of reflectors above reflector B is probably a record of these locally restricted turbidites. The primary characteristics of the B–I sequence of key reflectors include: (1) thin, distinct parallel reflections separated by acoustically transparent intervals; (2) prominent reflector pairs (B with C and D with E) underlain by relatively uniform spacing between E and F, F and G, and G and H; and (3) com-

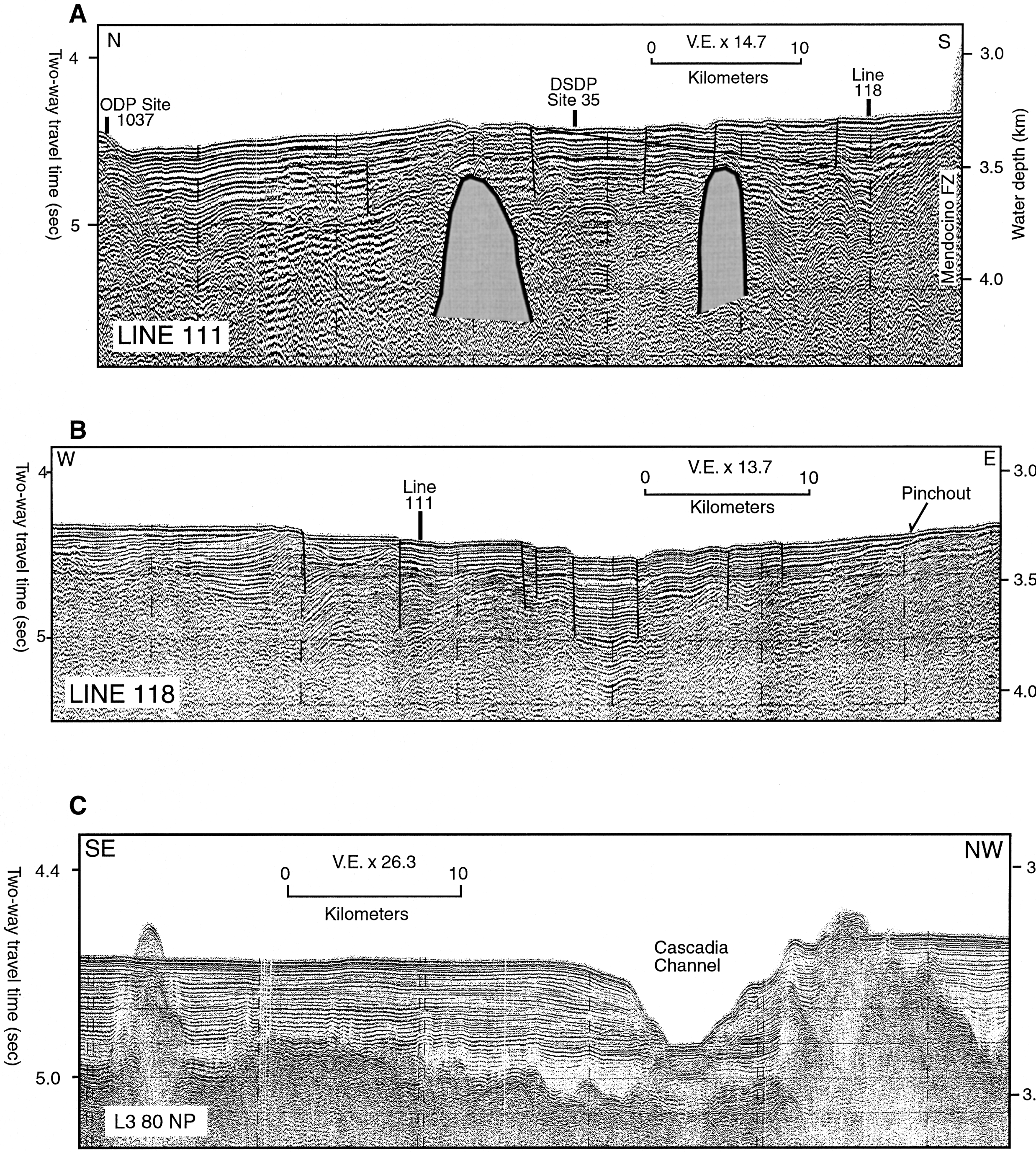

Figure 4. Seismic-reflection profiles (using an air-gun sound source) showing the extent of the sedimentary section north of the Mendocino Fracture Zone that includes the Escanaba Trough fill. See figure 1 for profile locations. *A*, Axial north-south profile extending from the vicinity of Site 1037 to the base of the Mendocino Fracture Zone at the south end; DSDP Site 35 is 800 m east of the line of the profile, and ODP Site 1037 is 3.7 km west. Intersection with profile (*line 118*) in *B* is shown. Probable fault offsets and volcanic intrusions (*gray pattern*) are shown. *B*, East-west profile across the mouth of the Escanaba Trough near the base of the Mendocino Fracture Zone. *C*, Profile across Cascadia Channel west of the area where overflow from the channel feeds turbidity currents southward toward the Mendocino Fracture Zone; see location in figure 1, inset.

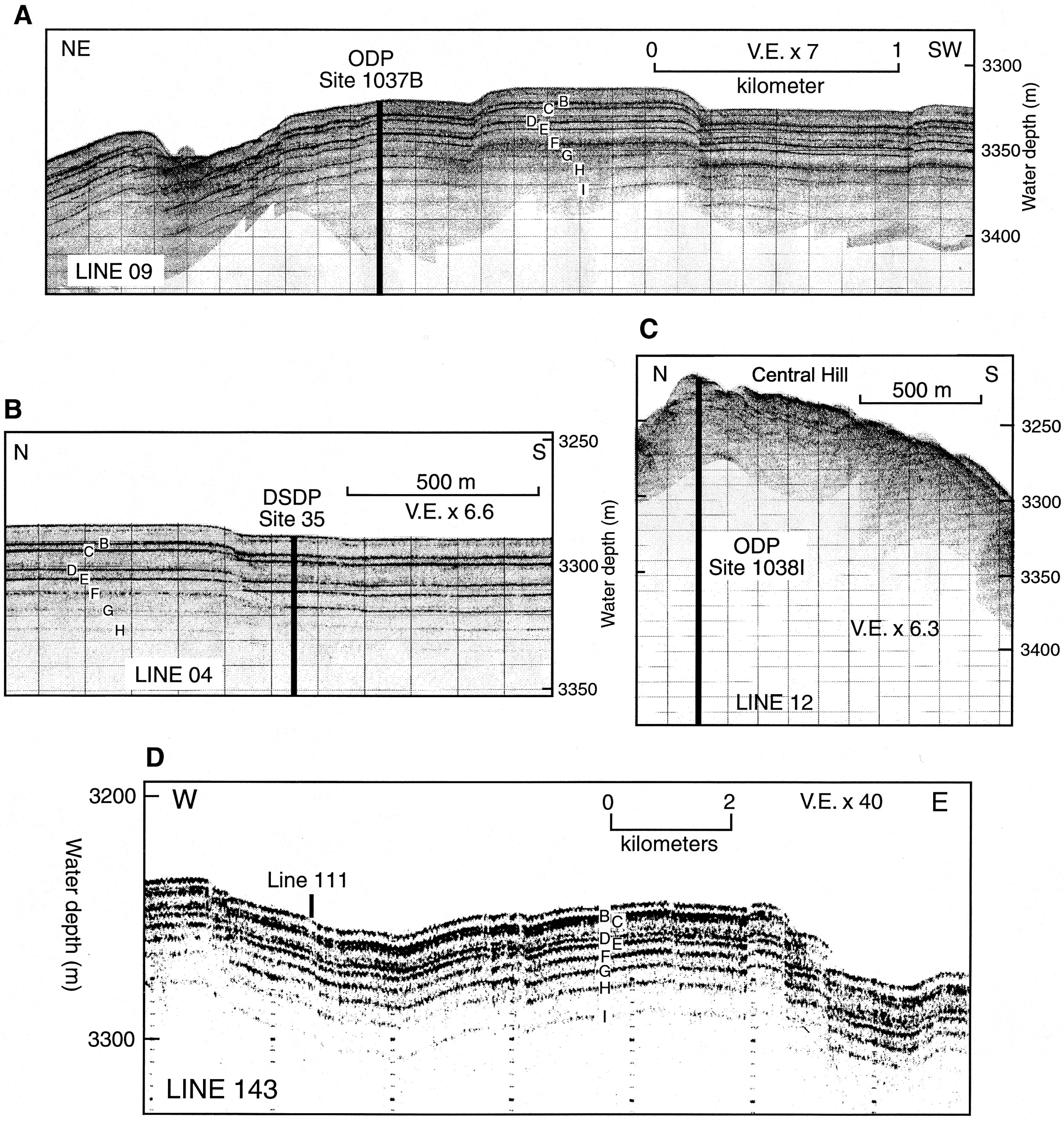

Figure 5. Deep-tow 4.5-kHz seismic-reflection profiles from the area of DSDP Site 35, ODP Sites 1037 and 1038, and surface-ship 3.5-kHz profile (*D*) from the southern limit of Escanaba Trough; see figure 1 for profile locations. *A*, Line ET 09 trends northeast-southwest through Site 1037 and shows a distinctive vertical spacing of reflectors that can be recognized throughout the profile length; the strongest and more laterally extensive reflectors are indicated by letters B–I; these key reflectors are correlated with the core data from Hole 1037B in figure 6. *B*, Line ET 04 is a north-south profile that passes 600 m west of DSDP Site 35; key reflectors B–H are present in the vicinity of the drill site. *C*, Line ET 12, which trends north-south, crosses line ET 09 and shows an undisturbed key reflector pattern at the south end; Hole 1038I, near the top of Central Hill, is at the north end of the profile. *D*, 3.5-kHz profile shows the same vertical pattern of reflections observed on the deep-tow images from the drill sites despite the more diffuse character of the reflectors caused by the much greater acoustic travel path for the surface-ship profile.

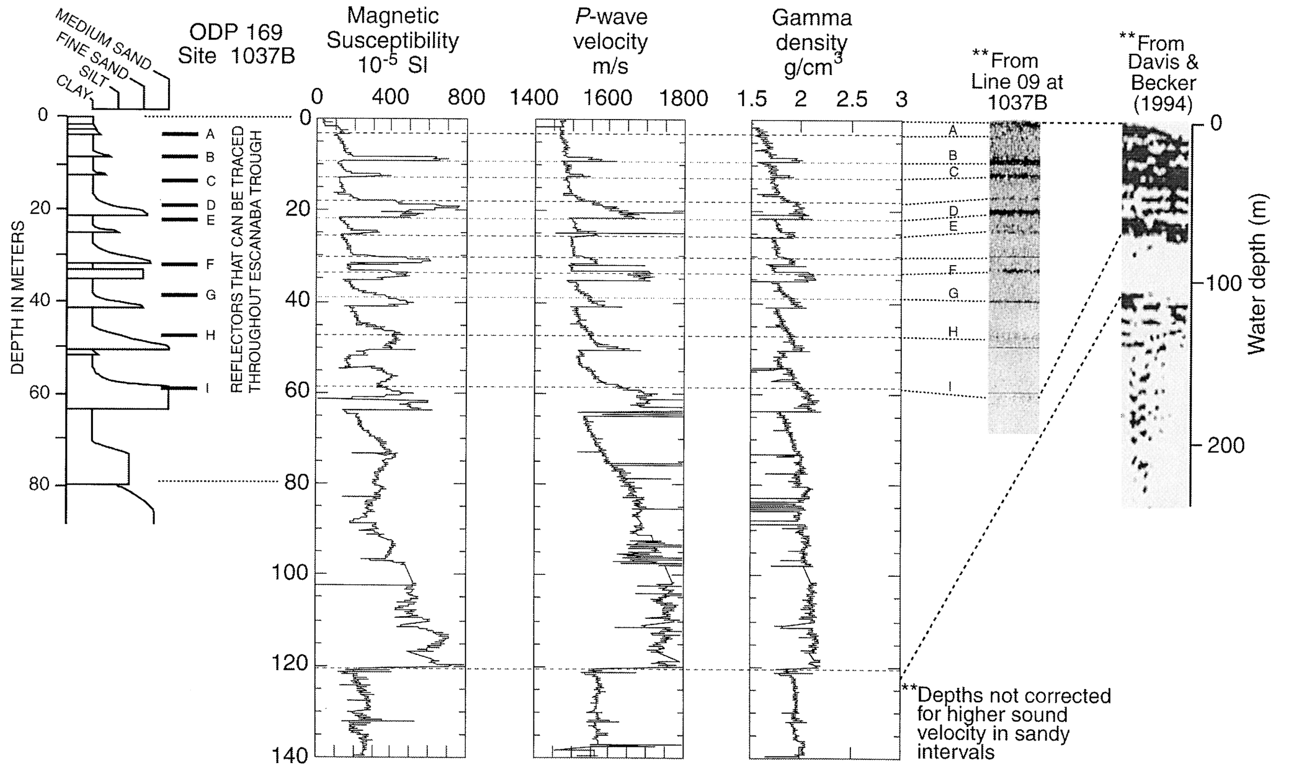

Figure 6. Correlation of the lithology, physical properties, and high-resolution 4.5-kHz profile from reference Hole 1037B. The lithologic log is from graphic sedimentation column (fig. 2) and the 4.5-kHz image is extracted from figure 5*A*. The logs for magnetic susceptibility, P-wave velocity, and gamma density are taken from the shipboard measurements using the Multi-Sensor Track (MST; fig. 17 in Shipboard Scientific Party 1998*c*). The basis of the correlation among the sediment log, MST logs, and 4.5-kHz profile is discussed in the text. The low-resolution seismic-reflection profile segment on the right side of the figure is extracted from line 3 of figure 3.3 in Davis and Becker (1994); the profile is in the vicinity of Hole 1037B.

mon occurrence on flat areas, slopes, and blocks separated by apparent faults (fig. 5*A*, 5*B*).

The observed range in water depth of the key reflector sequence suggests that the turbidity currents were at least 170 m thick after entering Escanaba Trough (Normark et al. 1997). The 4.5-kHz and deeper-penetration seismic-reflection profiles show that the turbidites of unit B can be mapped throughout the southernmost 75 km of Escanaba Trough (fig. 1). The volume of sediment deposited in the trough is shown in figure 3*B*. The total amount of sediment brought to the Pacific plate through Cascadia Channel is likely to be more than an order of magnitude greater than the volumes in Escanaba Trough because only the tops of the largest flows in Cascadia Channel could overflow to provide sediment in the trough.

Several of the deep-tow survey lines extend south to the area of DSDP Site 35; line ET 04 passes about half a kilometer west of DSDP Site 35 and shows the same distinct key reflector sequence (fig. 5*B*). The B-C and D-E pairs are especially distinct in this southern area, and the deepest reflector observed is H, about 43 mbsf. The sequence of key reflectors thus establishes a reasonably strong correlation between DSDP Site 35 and the reference Hole 1037B.

Part of the key reflector sequence (e.g., the two pairs of reflectors) is seen on the southern upper flank of Central Hill, where they are disrupted by minor faults. These observations can be used to provide a stratigraphic tie between the reference Hole 1037B and Hole 1038I.

Stratigraphic Correlations

Hole 1037B: Lithology, Reflection Profiles, and MST Log Profiles. The graded silt and sand megabeds in the interval between 1.68 and 63.60 mbsf (most of unit 2 in Shipboard Scientific Party 1998*b*) are well defined in several of the logged parameters from the Multi-Sensor Track (MST) (see fig. 6). The gamma density and P-wave velocity clearly record both the sharp basal boundary and the grading within individual turbidite beds. The magnetic susceptibility profile generally shows sharp bases for the beds but does not mimic the graded character as faithfully as the other two MST parameters. Very thin, graded silty mud beds, however, are well defined by the magnetic susceptibility but are difficult to detect in the velocity and density profiles (e.g., the two shallowest beds in unit B; figs. 2, 6).

The key reflectors B–I in the 4.5-kHz seismic-reflection profile that passes through Site 1037 clearly correlate with the turbidite beds (fig. 6). Reflectors B, C, and E correspond to the sharp bases of the turbidite beds, whereas D and the deeper reflectors, G, H, and I, correspond to the tops of graded sand intervals. It is not clear whether reflector F is from the base of the graded bed at 32 mbsf or from a thin underlying ungraded sand. Locally, the discontinuous reflector above F is probably from the upper part of the shallower, slightly coarser, and graded bed (fig. 6).

Below the turbidite bed identified as reflector I, there is a thick section of massive, poorly sorted sand in which no sedimentary structures survived the coring process (Shipboard Scientific Party 1998*b*). This sandy interval extends from 63.60 to 120.60 mbsf and makes up the bottom of unit 2 and all of unit 3 in the original shipboard description (lower part of unit B in this report). The MST log data, especially the velocity and density profiles, suggest that this interval might be one exceptionally thick-graded megabed (fig. 6).

The high-resolution 4.5-kHz profiles did not resolve any reflectors deeper than key bed I except on rift-valley terraces on the walls of the Escanaba Trough that stand >100 m above the axial valley floor. At the higher elevations, the total thickness of the key bed sequence (B–I) is thinner, but bedrock surfaces were observed beneath the sequence without any deeper turbidites (i.e., below reflector I). Seismic-reflection profiles across the northern Escanaba Trough, however, obtained by Davis and Becker (1994), show a distinct interval of no internal reflectors that appears to correspond to the lower part of unit B (fig. 6, right side). Above this acoustically transparent interval, there are numerous internal reflectors giving a signature that is typical for turbidite sediment. The observed reflection character for unit B in the Davis and Becker (1994) profiles is consistent with the interpretation that the lower 57 m of unit B represents a single depositional unit.

Correlation between Drill Sites. The key reflectors observed in the 4.5-kHz seismic-reflection profiles provide a compelling stratigraphic tie between reference Hole 1037B and DSDP Site 35, which was incompletely cored with the older drilling techniques and had poor recovery in many sections. The 4.5-kHz profiles also provide a tie between Holes 1037B and 1038I. The disruption of the key reflector pattern across the crest of Central Hill shown in figure 5*C* indicates a possible reason for the observation made by the Shipboard Scientific Party (1998*a*) that below about 100 mbsf the correlations among the nine holes at Site 1038 become more tenuous. The poor recovery between 78 and 257 mbsf in 1038I limits the correlation of the dominantly sandy section to the upper part of our unit B, which is the only interval effectively imaged by the 4.5-kHz profiles, and to the lower part of the section.

Petrography

Methods. Table 2 gives sample depths and types of analyses for cores that are included in this study (see fig. 2 for locations). The samples, which were collected from the more distinctly coarse-grained core intervals, were processed by wet sieving to remove the fraction finer than 62 μm in order to prepare thin sections of impregnated sand and the heavy-mineral grain mounts. Sand samples are generally very fine grained, in the range of 3–4 Ø, and only a few samples in the lower part of unit B are medium sand size. Point-counting procedures used the criteria proposed by Gazzi (1966) and Zuffa (1980, 1985, 1987) that minimize errors resulting from the dependence between grain size and rock composition. This approach to compositional analysis uses between 50 and 100 petrographic point-counting classes (table 3, available from *The Journal of Geology* office free of charge on request). From 300 to 400 grains were counted on thin sections stained for K-feldspar and used for the quartz-feldspar-lithics (QFL) classification. Grain counts of special heavy-mineral grain preparations (Gazzi et al. 1973, p. 26) were conducted by the ribbon method to tabulate different grain types (i.e., transluscents, opaques, turbids) in order to identify about 200 transluscent grains from each sample (table 4, available from *The Journal of Geology* office free of charge on request). The fraction examined has a grain density >2.96 g/cc (tetrabromoethane) and a size range of 0.25–0.0625 mm.

Gross Composition. The sand samples are feldspatholithic to lithic and fall in the dissected and transitional subfields of the "magmatic arc" field of Dickinson (1985; fig. 7*A*). The recalculated light

Table 2. Summary of Samples Analyzed for Gross Composition and Heavy Minerals from Ocean Drilling Program Leg 169, Holes 1037B and 1038I

Sample number	Core and Section	Sampled interval (cm)	Gross composition	Heavy minerals	Depth below sea floor (m)
9	3H-03	57-61	–	×	19.69
11	3H-04	82-85	×	–	21.44
14	4H-CC	6-8	×	×	35.42
16	6H-05	7-9	×	–	50.68
18	7H-CC	8-10	×	×	63.97
21	9H-07	66-70	×	–	82.78
22	10H-02	115-120	×	–	85.27
24	12H-04	18-23	×	×	106.31
25	13H-03	118-122	×	–	115.30
26	15H-01	0-2	–	×	130.11
29/29a	17H-07	50-62	–	×	158.66
30	18H-07	36-41	–	×	167.99
31	19H-06	7-10	×	–	175.43
33/33a	21X-CC	26-35	–	×	182.81
34	22X-02	100-102	×	×	194.71
39	27X-01	15-20	×	–	240.38
40/40a	29X-02 29X-02	118-123 130-136	–	×	262.17
40b	32X-05	120-126	–	×	294.19
51a	42X-02	10-16	×	×	385.93
52	42X-04	73-75	–	×	389.54
53	43X-CC	13-18	×	×	403.49
54	44X-02	126-132	–	×	406.39
54a	45X-CC	23-29	×	×	418.56
57/57a	49X-06 49X-07	146-148 6-8	×	×	460.61
61/61a	53X-01 53X-CC	49-51 24-30	×	×	491.24
96	1X-01	29-31	×	–	0.30
97	1X-01	125-127	×	–	1.26
104	5H-CC	12-14	×	×	45.69
107	8X-02	27-31	×	–	66.60
108	9X-02	124-126	×	×	77.15
109	12X-01	6-8	×	–	103.27
110	16X-CC	8-10	×	×	141.79
110a	21X-01	14-20	×	×	189.87
111/111a	28X-04	135-142	–	×	262.99
113/113a	30X-03	8-13	×	×	279.00
114	31X-01	83-87	–	×	286.95
119/119a	36X-01	35-44	×	×	334.49

Note. Samples from 9 to 61/61a are from Hole 1037B; samples from 96 to 119/119a are from Hole 1038I. A cross indicates analyzed; a minus, not analyzed.

and heavy mineral average composition of modern sand from deposits of the Columbia River analyzed by Whetten et al. (1969, p. 1160; i.e., Q 42%, F 27%, L 31%; orthopyroxene 11%, clinopyroxene 31%, amphibole 42%) closely matches that of the Escanaba Trough sand turbidites. A few samples plot outside of the main cluster in the "continental block" and "undissected arc" subfields. One sample is uncommonly mica rich (sample 53), and three arkosic samples (14, 17a, and 17b: see Zuffa et al. 1997, table 2) are strongly affected by diagenesis. The sand samples generally contain an abundant volcanic component with high plagioclase/K-feldspar (P/K) ratios (fig. 7*B*) and lithic-volcanic/lithic-sedimentary ratios (fig. 7*C*). The feldspar component consists mostly of pristine plagioclase (andesine-labradorite) and minor sericitized K-feldspar, including rare microcline and fresh sanidine. The unaltered plagioclase grains that have the same mineralogical and textural features as the plagioclase observed in the phenocrysts of the volcanic rock fragments have been distinguished as "pristine plagioclase" during point counting. The mafic volcanic component consists mainly of perlitic brown glass (commonly chloritized), porphyritic grains with aphanitic or brown vitric groundmass, plagioclase, clinopyroxene, orthopyroxene, hornblende phenocrysts, and Fe-Ti oxides. Volcanic grains of intermediate composition show a plagioclase microlithic texture with rare pyroxene and opaque minerals. Acidic volcanic grains include pristine glass, glass shards, and pumices, colorless or brownish grains with vitric and felsitic texture, some containing microphenocrysts of plagioclase, quartz,

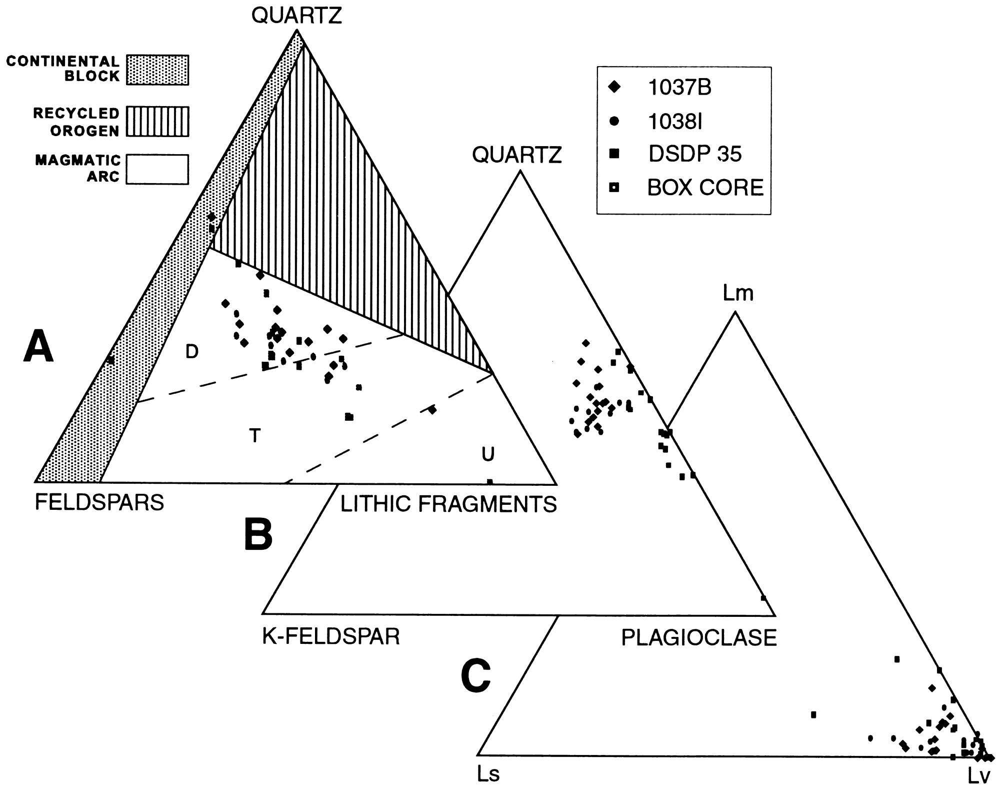

Figure 7. Classification of the light-mineral sand fraction integrated for DSDP Site 35 and Holes 1037B and 1038I. *A*, *U* = undissected arc, *T* = transitional arc, *D* = dissected arc (Dickinson 1985). *C*, *Lv* = lithic volcanics, *Lm* = lithic metamorphic, *Ls* = lithic sedimentary (including calcite monocrystals). Samples indicated as DSDP 35 and box core are from Zuffa et al. (1997).

and rare K-feldspar. K-feldspar is also locally present as a constituent of the groundmass of felsitic grains. The nonvolcanic fine-grained rock-fragment component is made up of low-grade phyllite and slate grains in trace quantities. The coarse-grained rock fragments are represented by rare granitoid and gneiss.

Unworn tests and/or fragments of foraminifers are generally present in low amounts. A few samples contain significant quantities of spheroidal to oblate clayey grains that show internal brownish-dull halos, which are carbon and phosphorous rich and that mimic the grain contour. These grains are tentatively interpreted as fecal pellets representing intrabasinal grains ripped up by the turbidity currents and subsequently deposited in the coarse-grained intervals at the base of the turbidite beds.

Volcanic rock fragments make up more than one-third of the sand component of the Escanaba Trough sediment and are by far the most abundant constituents of the fine-grained lithic fraction (fig. 7*C*). If pristine plagioclase and sanidine are added to the volcanic rock fragment component, the result is that more than half of the sand grains of the Escanaba Trough sediment fill are derived from volcanic sources. The QFL plot (fig. 7*A*) shows little variation in the Q/F ratio. In contrast, variations in the fine-grained rock-fragment contents show scatter of the samples from the QF side to the L vertex of the triangle. The down-hole distribution of the $V/(Q + F + V)$ ratio integrated for ODP Holes 1037B and 1038I and DSDP Site 35 (fig. 8) shows that the volcanic component in the upper 180 m of the section is generally higher than in the lower portion of the section.

Heavy Minerals. The heavy-mineral assemblage is mainly characterized by amphiboles (brown and green, blue-green hornblende, basaltic hornblende, and actinolite), clinopyroxene (augite and titanaugite), orthopyroxene (bronzite and hypersthene), and epidotes (clinozoisite/epidote). Garnet and titanite are present in almost all samples but in variable amounts. Other characteristic minerals such as allanite, zoisite, olivine, chloritoid, staurolite, glaucophane, sillimanite, kyanite, andalusite, monazite, spinel, and apatite occur irregularly in small

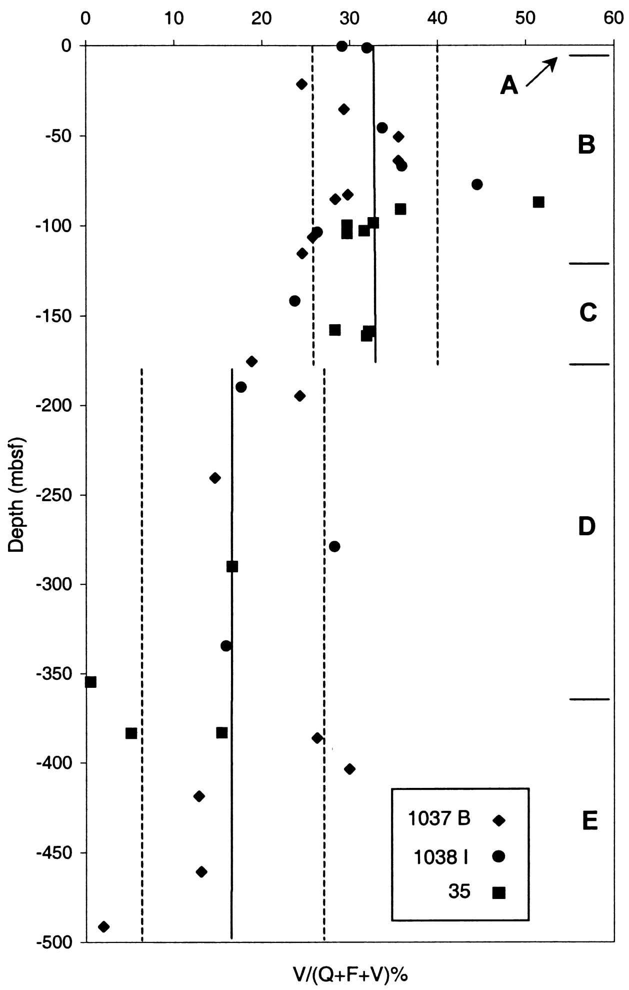

Figure 8. Down-hole distribution of the volcanic component integrated for Holes 1037B and 1038I (this study) and DSDP Site 35 (Zuffa et al. 1997). V = volcanic grains, Q = quartz; F = feldspars. Dashed lines indicate the standard deviation (1σ).

or in trace amounts. Barite and mesitite occur locally, mostly as authigenic minerals. Some pyroxene and amphibole grains show distinct corrosion features, resulting from postdepositional dissolution phenomena (see also Zuffa et al. 1997, fig. 6*E*).

The down-hole heavy-mineral distribution in ODP Hole 1037B shows a transition from an amphibole/clino-orthopyroxene assemblage to an amphibole-rich ± minor pyroxene assemblage to an amphibole-rich assemblage (fig. 9). The deepest 30 m of sediment that overlies the basalt at 507.8 mbsf exhibits a garnet-epidote association. The sand samples from Site 35 and Hole 1038I show the same trends; however, there are samples characterized only by the garnet-epidote assemblage that occur at shallower depths (i.e., samples at 141.8, 189.9, and 236.0 mbsf), which at Hole 1038I is consistent with a greater degree of hydrothermal alteration as expected because of the known near-surface sulfide mineralization.

Discussion

To understand the conditions that produce the young, thick sediment fill within Escanaba Trough,

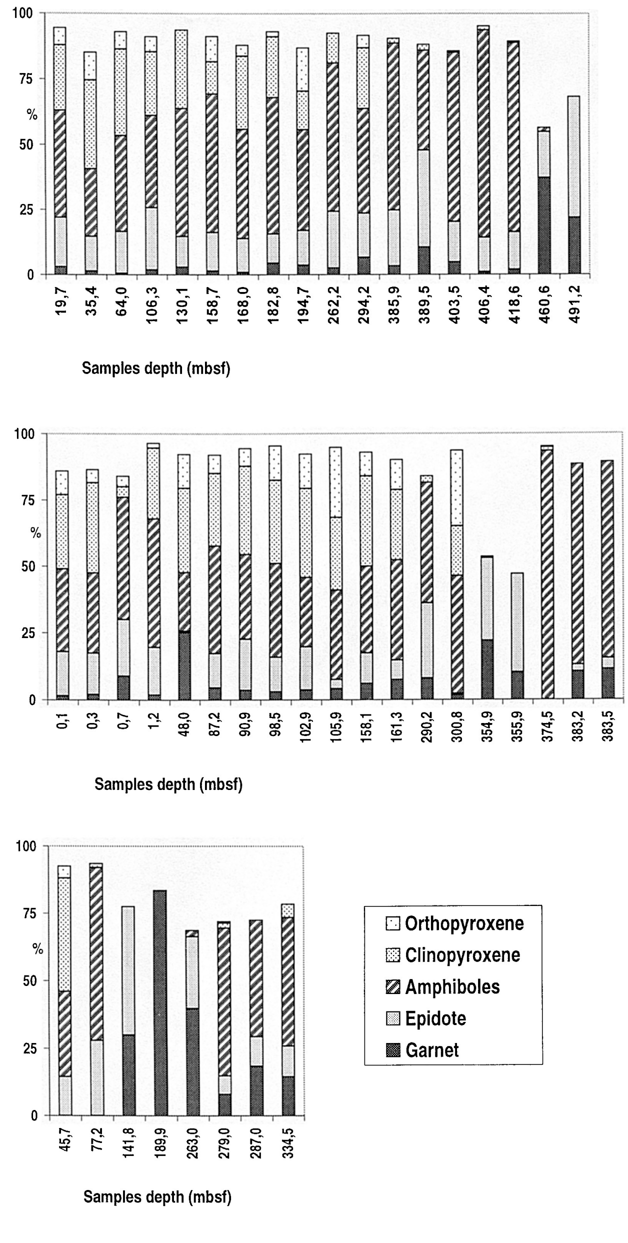

Figure 9. Down-hole distribution of garnet, epidote, amphibole, and clino- and orthopyroxene for Hole 1037B (*upper*), DSDP Site 35 (*middle*; taken from Vallier et al. 1973; Zuffa et al. 1997) and 1038I (*lower*).

we will (1) discuss the provenance of the turbidite sand, (2) evaluate the probable pathway(s) for the turbidity currents to reach the axial valley, and (3) speculate on the flow processes. The processes that apply to the upper part of the sequence in the reference Hole 1037B (from the sea floor to 120 mbsf), for which there is good seismic-stratigraphic correlation with Site 35 and 1038, can be used to evaluate the depositional history for the lower part of the sediment sequence in the axial valley, for which there is a weaker correlation.

Provenance. Most of the sand-sized material recovered from the turbidite fill of the Escanaba Trough at DSDP Site 35 is clearly from the North American continent (Vallier et al. 1973; Zuffa et al. 1997). In spite of the high relief of the Mendocino Fracture Zone just south of the Escanaba Trough, this source area can be easily ruled out because of its oceanic-crust lithology, which does not match with the gross sand composition characterized by significant amounts of quartz, K-feldspar, andesitic to rhyolithic rock fragments, and granitic rocks.

Vallier et al. (1973) and Zuffa et al. (1997) studied the composition of the Escanaba Trough sands from DSDP Site 35 although it was cored discontinuously (fig. 2). Studies of the sand fraction from DSDP Site 35 distinguished two different petrofacies for the source rocks: (1) a facies of lithic arkoses to litharenites with amphibole and pyroxene in the upper part of the sediment fill, and (2) a facies of arkose with only amphibole in the lower part of the fill. On this basis, the authors related the upper petrofacies to the Columbia River drainage basin, while the lower assemblages were related to the Klamath River source of northern California.

The new data from the samples collected in Holes 1037B and 1038I are entirely consistent with the results of Vallier et al. (1973) and Zuffa et al. (1997) for the upper part of the section. The results from this study, however, suggest a reinterpretation of the lower part of the section because the composition of the light fraction is not only arkosic but some samples are litharenitic. In addition, the distribution of heavy minerals in Hole 1037B (fig. 9) shows a down-hole transition from amphibole/clino-orthopyroxene assemblage to amphibole/clinopyroxene assemblage to an amphibole-rich assemblage, and finally to an epidote-garnet assemblage at the bottom of the section. The epidote-garnet assemblage also occurs in several samples from the intermediate part of Hole 1038I (fig. 9) that is affected by severe hydrothermal alteration (Shipboard Scientific Party 1998*a*). This observation suggests diagenetic changes within the heavy-mineral component in the section and further indicates an increasing effect of intrastratal dissolution with subbottom depth (e.g., Scheidegger et al. 1973). The data indicate that the effects of the hydrothermal fluids reach a maximum in the permeable intervals of the section (samples at 141.8 and 189.9 mbsf, table 2).

The trends noted above (i.e., the down-hole change of the amphibole/clino-orthopyroxene association to an amphibole-rich association) are most likely related to diagenesis and not to differences in the sediment-source areas. The down-hole distribution of the $V/(Q + F + V)$ ratio for ODP Holes 1037B and 1038I and DSDP Site 35 (fig. 8) shows that the volcanic component in the upper part of the section is generally higher than in the lower part of the section. Sediment from the upper 177.60 m of the section (fig. 2) is related to the stages of Wisconsinan deglaciation. It can be observed that a significant amount of sand derived by pyroclastic fall, surge, and flow volcanic activity was likely deposited and stored within the glaciers during the Wisconsinan ice accumulation phases when onland erosion was necessarily limited and volcaniclastic grains were the only clastic sediment available. During deglaciation this sand was then released, thus increasing the content of the volcanic component of the discharged sediment. We conclude that a distinct terrigenous supply from the northern California rivers is not demonstrated, and the bulk of the Escanaba Trough sediment is mostly derived from the Columbia River drainage basin.

Pathway. The simplest pathway to envision for the transportation of sediment from the mouth of the Columbia River to the Escanaba Trough is to assume southward flow along the base of the continental slope. A generally southerly trending channel (the Astoria Channel) on the Astoria fan extends from near the fan apex, which is close to the Columbia River mouth, south to about the Blanco Fracture Zone (fig. 1, inset). The average rate of deposition for Pleistocene turbidites at DSDP Site 174, which lies on a broad levee about 35 km west of the axis of Astoria Channel, is about 0.25 m/k.yr. (Shipboard Scientific Party 1973). This average rate is more than an order of magnitude less than those for units B through D (as defined in this report) in Escanaba Trough (fig. 3*A*). Recent work has shown that the Astoria channel formerly continued south across the Blanco Fracture Zone. Wolf et al. (1999) compiled available seismic-reflection data from the Gorda plate and found that the Astoria channel extended almost to the Mendocino Fracture Zone, but it is now sediment filled for most of its length south of 44°N. New multibeam bathymetric data indicate that the Astoria channel has been blocked by the Heceta megaslump that occurred about 110 ka (Goldfinger et al. 2000). The age of the Heceta failure, therefore, substantially predates deposition of the section recovered at reference Hole 1037B.

The compilation of 3.5-kHz seismic-reflection profiles as part of the study by Wolf et al. (1999) did not record deposits showing an acoustic character similar to that of the upper 60 m of sediment at Hole 1037B (S. Wolf, pers. comm., 1998). Because the thickness of the turbidity-current flow in the Escanaba Trough was at least 170 m (Normark et al. 1997), it is likely that some record of the passage of the flows should have been left on the Gorda plate south of the Blanco Fracture Zone if the Astoria channel had been the main pathway to the Escanaba Trough and if turbidity currents from the Astoria Channel were not blocked by the Heceta slump.

ODP Site 1020 is on a small hill about 100 m high that lies along the west side of the Astoria channel trace on the Gorda plate (fig. 1, inset). A few graded, sandy silt beds were recovered in the upper 15 m during coring at this site, but there were no thick turbidite sand beds (Shipboard Scientific Party 1997). The average sedimentation rate at this site is 0.1 m/k.yr., which is about two orders of magnitude less than the deposition rate in Escanaba Trough. Turbidity currents as thick as those that entered the Escanaba Trough would be expected to have left more sediment on the hilltop that stands only about 100 m above the channel. In addition, Site 1020 is on the right-hand side (looking downchannel) of the trace of Astoria channel, and the effects of the Coriolis force would have resulted in thicker flow on the right side. Finally, the petrography of the sand grains in two beds at Site 1020 from 0.80 mbsf and 2.47 mbsf are more consistent with a source from a northern California river (G. G. Zuffa and F. Serra, unpub. data).

The evidence presented above is mostly circumstantial and does not preclude the possibility that turbidity currents generated offshore of the Columbia River might have flowed south along the margin; there is, nevertheless, little observational support for this eastern pathway.

The seismic-reflection data (e.g., fig. 4*B*) show that the sediment fill of the Escanaba Trough at its intersection with the Mendocino Fracture Zone wedges out to the east. Available high-resolution 3.5-kHz reflection profiles show that the sequence of key reflectors seen in the deep-tow records from the northern part of the Escanaba Trough can be recognized along the same tracklines depicted in figure 4*A* and 4*B* (fig. 5*B* and 5*D*, respectively). Similar to the reflector geometry seen in the deeper penetration air-gun profile of figure 4*B*, the 3.5-kHz data at the southern end of the Escanaba Trough shows that the key reflector sequence in the upper part of the section thins eastward and becomes unrecognizable. Locally, the lateral equivalent to the key reflector sequence appears to onlap sediment of the Gorda plate to the east.

West of the Escanaba Trough, the sediment accumulation locally exceeds that along the axis of the rift valley. The key reflector sequence, however, is not unequivocally recognized west of longitude 128°W. Normark and Reid (1998) show that the thick sediment accumulations along the northern flank of the Mendocino Fracture Zone are contiguous with the Tufts fan and abyssal plain to the north (fig. 1). The apex of the Tufts fan is near the current exit of the Cascadia Channel from the Blanco Fracture Zone. Long-range side-looking sonar images show patterns similar to channel and lobe features that have been described from large modern turbidite systems (Normark and Reid 1998). The backscatter pattern on the side-looking sonar images indicates southerly dispersal of sediment.

The seismic-reflection and side-looking sonar data available from the western flank of Gorda Ridge provide reasonable evidence for concluding that the main pathway for turbidity currents flowing to the Escanaba Trough was on the Pacific plate (fig. 10). The pebble-grade sediment with an eastern Washington provenance that was recovered from Cascadia Channel west of the Blanco Fracture Zone (Griggs et al. 1970) suggests that overflow from the Cascadia Channel near its exit from the Blanco Fracture Zone deposited turbidite sediment on the Tufts fan and that part of the flows continued south, where they were deflected eastward by the Mendocino Fracture Zone before being intercepted by the axial rift in the Escanaba Trough. The Cascadia channel at the point of overflow to the Tufts fan is >200 m deep; immediately to the west of Tufts fan, the channel is observed to be deeply eroded into the turbidite sequence of the Tufts Abyssal Plain (fig. 4*C*). The relief of the Cascadia Channel suggests that only the largest turbidity currents could overflow onto Tufts fan and provide a source for Escanaba Trough fill. Thus, even if all the Lake Missoula flood events resulted in hyperpycnally generated turbidity currents, only the largest of these would be recorded in Escanaba Trough.

Missoula Floods. The age of the graded sand beds from the upper 120 m (unit B) of the reference Hole 1037B and the sediment source in eastern Wash-

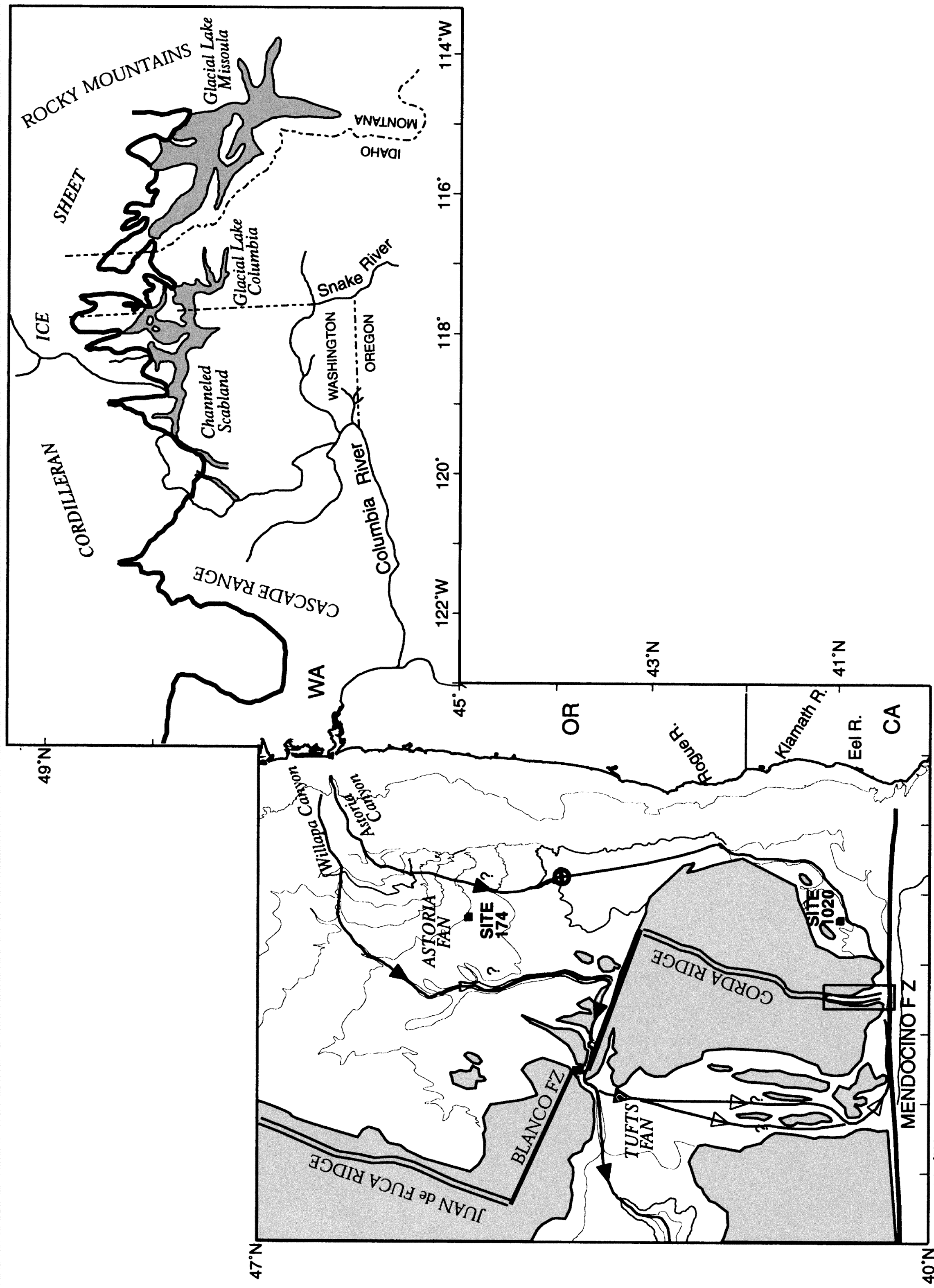
ROCKY MOUNTAINS
Glacial Lake Missoula
MONTANA
IDAHO
SHEET
ICE
CORDILLERAN
Glacial Lake Columbia
Channeled Scabland
Snake River
WASHINGTON
OREGON
Columbia River
CASCADE RANGE
WA
114°W
116°
118°
120°
122°W
49°N
45°
43°N
41°N
OR
CA
Rogue R.
Klamath R.
Eel R.
124°W
127°
130°W
47°N
40°N
Willapa Canyon
Astoria Canyon
ASTORIA FAN
SITE 174
SITE 1020
GORDA RIDGE
MENDOCINO F Z
BLANCO FZ
TUFTS FAN
JUAN de FUCA RIDGE

ington suggest that the Escanaba Trough megaturbidites of unit B are the result of the late Wisconsinan catastrophic floods from glacial Lake Missoula (fig. 10). Although several aspects are still unsolved in the history of the Channeled Scabland after almost a century of controversy, several lines of evidence from the voluminous published literature (reviewed by Baker and Bunker 1985), recent paleomagnetic data (Steele 1991), studies on loess deposits (McDonald and Busacca 1988), studies of mammal fossils (Spencer 1989), ages of tephra layers (Crandell et al. 1981), and mathematical models (Clarke et al. 1984) support the idea that Lake Missoula, in late Wisconsin time, released a number of glacial outburst floods, or jökulhlaups. Waitt (1985) and Atwater (1986) support the hypothesis that a large number of Missoula floods (40–89) occurred in a time interval of 2000–2500 yr (between 15.3 and 12.7 ka; Waitt 1985). Baker and Bunker (1985), O'Connor and Baker (from hydraulic calculation; 1992) and Shaw et al. (1999), all in agreement with Bretz (1969), argue for one very large cataclysmic flood in late Wisconsin time, which could eventually have been followed by later, smaller floods.

Unit B is a fining- and thinning-upward sequence of turbidite sand beds with very few thin hemipelagic interbeds (fig. 2). The lowermost 57 m of unit B consists of >80% sand, including 5% medium- to very coarse-grained sand (2–0.25 mm), which is unusual in the entire section. There are no lithologic variations in this interval, except for grading in the upper 17 m. The soupy nature of most of the recovered sand precludes a firm interpretation, but the lack of mud or clay chips indicates there probably were no breaks in this sandy interval, suggesting that it can be interpreted as a single megaturbidite bed or a series of amalgamated thick turbidite beds. Additional evidence that this thick sandy interval may be a single depositional unit is the lack of internal reflectors in profiles from the northern part of the Escanaba Trough (Davis and Becker 1994). Our age determinations from on top of and immediately below this interval are 15,750 ± 70 and 15,482 ± 100 yr, respectively, consistent with very short-lived, single-event deposition.

The upper half of unit B forms a distinct fining- and thinning-upward sequence of about 10 graded beds ranging from 12 to 3.5 m thick (fig. 2). This part of unit B corresponds to the key reflector sequence that can be traced throughout the Escanaba Trough. Key reflector C overlies a thin hemipelagic mud dated at 10,882 ± 85 yr. This implies that the upper part of unit B was deposited in <5 k.yr.

Atwater (1987, p. 185) reports a ^{14}C age of 14,490 ± 290 yr from detrital wood found near the middle of a 115-m-thick glaciolacustrine section consisting of varved intervals of 15–55 beds interstratified with graded beds near Manila Creek, which is a tributary to the Sanpoil River of glacial Lake Columbia. This glaciolacustrine deposit contains 89 beds that have been related to the Missoula floods of Fraser age. It has been suggested that if flood-bed thickness and grain size are proportional to flow discharge, then there is a trend toward smaller events through time for the Missoula floods (fig. *3B*; Waitt 1980; Atwater 1986, 1987; Smith 1993).

Below unit B, there is a lithologically similar sequence that is 57 m thick and fines upward. About 35 m of sand at the base of unit C appears to comprise three turbidite beds that fine upward to mud turbidite beds with a thin fine-grained sandy base. The top of unit C is 15,482 ± 100 yr old, and the base is younger than 25 ka, based on the date from the middle of unit D. Unfortunately, no date was obtained from the basal part of the unit, but we suggest that the thinning- and fining-upward sequence of unit C could record earlier jökulhlaups from the Columbia River drainage area.

The observations above suggest that the unit B and perhaps the unit C sequences of graded beds represent the deep-sea sedimentary record of the Lake Missoula glacial outburst floods. The floods entered the ocean close to the heads of Astoria and Willapa Canyons (fig. 10) when sea level was about 60–70 m below present. The exceptionally high discharge rate and sediment load of many of the Missoula events were likely to have generated hyperpycnal gravity flows (Mulder and Syvitski 1995; Mutti et al. 1996). The largest of these events generated turbidity currents that were capable of reaching the Escanaba Trough.

Figure 10. Schematic map showing glacial Lakes Missoula and Columbia and the probable submarine pathways to Escanaba Trough for sediment carried by floods from the glacial lakes after passing through the Columbia River drainage basin. Offshore bathymetry modified from Grim et al. (1992) and subaerial features from Baker and Bunker (1985); bold line indicates edge of the Cordilleran ice sheet.

Unit D consists of thick-bedded muddy turbidites locally with fine sand bases. A sedimentation rate of 7.6 m/k.yr. was calculated from two ages in the unit, 24,982 and 32,182 yr at 262.25 and at 316.90 mbsf (table 1), respectively, which is slower than that of the overlying sandier units B and C. If a similar rate of sedimentation characterizes the lower part of unit D, then the bottom of the unit at 366 mbsf would be about 40 ka. Unit D and unit E, which is slightly sandier than unit D, probably were deposited during oxygen isotope stage 3 (Martinson et al. 1987), when sea level was lower than at present and more variable.

Conclusions

Depositional geometry, high-resolution stratigraphy, and sand composition indicate that the oceanic rift-valley sedimentary fill of the Escanaba Trough was derived dominantly from the Columbia River. This sediment reached the Escanaba Trough through the Cascadia Channel and the Tufts abyssal plain, flowing along the north flank of the Mendocino Fracture Zone ridge and entering the oceanic rift valley flowing toward the north (fig. 10). Two fining- and thinning-upward turbidite sequences (units B and C), which together are 175 m thick, were cored below the thin surficial Holocene hemipelagic interval of mud. The two sequences have AMS ^{14}C ages from 16 to 11 ka and a deposition rate from 9 m/k.yr. to essentially instantaneous (fig. 3*A*). The type of sequence and the composition of sand, age, and deposition rate suggest that these turbidite beds were derived from the Lake Missoula outbursts during Wisconsinan deglaciation. Many of the jökulhlaups from the glacial lakes continued flowing as hyperpycnally generated turbidity currents on entering the sea at the mouth of the Columbia River and were able to reach the oceanic ridge valley of the Escanaba Trough, resulting in a submarine transport path of >1100 km.

ACKNOWLEDGMENTS

The financial support for G. Zuffa was provided by the National Council of Research (CNR 96.00286 CT 05, 97.00268 CT 05). Radiometric analyses were performed by the National Ocean Sciences Accelerator Mass Spectrometry Facility at Woods Hole (National Science Foundation Cooperative Agreement OCE-9301015) and the Eidgenössische Technische Hochschule at Zürich. The Joint Oceanographic Institutions/U.S. Science Support Program funded work by C. Brunner. We thank J. A. Reid for assisting with preparation of figure 1. The manuscript has benefited from reviews by F. L. Wong and H. E. Clifton. We would like to thank V. R. Baker, B. F. Atwater, and an anonymous reviewer, whose comments greatly strengthened this article. This article is University of Southern Mississippi Department of Marine Science Contribution 195. This article is one of the primary contributions by C. Brunner and G. Zuffa for the ODP Leg 169.

REFERENCES CITED

Atwater, B. F. 1986. Pleistocene glacial-lake deposits of the Sanpoil River Valley, northeastern Washington. U.S. Geol. Surv. Bull. 1661.

———. 1987. Status of glacial Lake Columbia during the last floods from glacial Lake Missoula. Quat. Res. 27: 182–201.

Baker, V. R., and Bunker, R. C. 1985. Cataclysmic late Pleistocene flooding from glacial Lake Missoula: a review. Quat. Sci. Rev. 4:1–41.

Bretz, J. H. 1969. The Lake Missoula floods and the Channeled Scabland. J. Geol. 77:505–543.

Brunner, C. A.; Normark, W. R.; Zuffa, G. G.; and Serra, F. 1999. Deep-sea sedimentary record of the late Wisconsin cataclysmic floods from the Columbia River. Geology 27:463–466.

Carlson, P. R., and Nelson, C. H. 1987. Marine geology and resource potential of Cascadia Basin. *In* Scholl, D. W.; Grantz, A.; and Vedder, J. G., eds. Geology and resource potential of the continental margin of western North America and adjacent ocean basins—Beaufort Sea to Baja California. Circum-Pacific Council for Energy and Mineral Resources, Earth Science Series 6:523–535.

Clarke, G. K. C.; Mathews, W. H.; and Pack, R. T. 1984. Outburst floods from glacial Lake Missoula. Quat. Res. 22:289–299.

Clarke, S. H., Jr. 1987. Geology of the California continental margin north of Cape Mendocino. *In* Scholl, D. W.; Grantz, A.; and Vedder, J. G., eds. Geology and resource potential of the continental margin of western North America and adjacent ocean basins—Beaufort Sea to Baja California. Circum-Pacific Council for Energy and Mineral Resources, Earth Science Series 6:337–351.

Crandell, D. R.; Mullineaux, D. R.; Rubin, M.; Spiker, E.; and Kelly, M. L. 1981. Radiocarbon dates from volcanic deposits at Mount St. Helens, Washington. U.S. Geol. Surv. Open-File Rep. 81-844.

Davis, E. E., and Becker, K. 1994. Thermal and tectonic structure of Escanaba Trough: new heat-flow measurements and seismic-reflection profiles. *In* Morton, J. L.; Zierenberg, R. A.; and Reiss, C. A., eds. Geologic, hydrothermal, and biologic studies at Escanaba Trough, Gorda Ridge, offshore northern California. U.S. Geol. Surv. Bull. 2022, p. 45–64.

Dickinson, W. R. 1985. Interpreting provenance relations from detrital modes of sandstones. *In* Zuffa G. G., ed. Provenance of arenites, NATO-ASI. Dordrecht, Reidel, p. 333–361.

Fouquet, Y.; Zierenberg, R. A.; Miller, D. J., et al. 1998. Proc. Ocean Drilling Program, Init. Rep. 169. College Station, Tex., 592 p.

Gazzi, P. 1966. Le arenarie del flysch sopracretaceo dell'Appennino modenese: correlazioni con il flysch di Monghidoro. Mineral. Petrogr. Acta 12:69–97.

Gazzi, P.; Zuffa, G. G.; Gandolfi, G.; and Paganelli, L. 1973. Provenienza e dispersione litoranea della sabbie delle spiagge adriatiche fra le foci dell'Isonzo e del Foglia: inquadramento regionale. Soc. Geol. Ital. Mem. 12:1–37.

Goldfinger, C.; Kulm, L. D.; and McNeill, L. C. 2000. Super-scale failure of the southern Oregon Cascadia margin. Pure Appl. Geophys., in press.

Griggs, G. B.; Kulm, L. D.; Waters, A. C.; and Fowler, G. A. 1970. Deep-sea gravel from Cascadia Channel. J. Geol. 78:611–619.

Grim, M. S.; Chase, T. E.; Evenden, G. I.; Holmes, M. C.; Normark, W. R.; Wilde, P.; Fox, C. G.; Lief, C. J.; and Seekins, B. A. 1992. Map showing bottom topography of the Pacific continental margin, Strait of Juan de Fuca to Cape Mendocino. U.S. Geol. Surv. Misc. Investig. Ser. Map I-2091-C.

Hurley, R. J. 1960. The geomorphology of abyssal plains in the northeast Pacific Ocean. Marine Physical Laboratory, Scripps Institution Oceanography Reference 60–7, 105 p.

———. 1964. Analysis of flow in Cascadia deep-sea channel. *In* Miller, R. L., ed. Papers in marine geology. New York, Macmillan, p. 117–132.

Karlin, R., and Lyle, M. 1986. Sediment studies on the Gorda Ridge. Oreg. Dep. Geol. Miner. Ind. Open-File Rep., 0-86-19, 76 p.

Koski, R. A.; Benninger, L. M.; Zierenberg, R. A.; and Jonasson, I. R. 1994. Composition and growth history of hydrothermal deposits in Escanaba Trough, southern Gorda Ridge. *In* Morton, J. L.; Zierenberg, R. A.; and Reiss, C. A., eds. Geologic, hydrothermal, and biologic studies at Escanaba Trough, Gorda Ridge, offshore northern California. U.S. Geol. Surv. Bull. 2022, p. 293–324.

Martinson, D. G.; Pisias, N. G.; Hays, J. D.; Imbrie, J.; Moore, T. C., Jr.; and Shackleton, N. J. 1987. Age dating and the orbital theory of the ice ages: development of a high-resolution 0 to 300,000-year chronostratigraphy. Quat. Res. 27:1–29.

McDonald, E. V., and Busacca, A. J. 1988. Record of prelate Wisconsin giant floods in the Channeled Scabland interpreted from loess deposits. Geology 16:728–731.

McMurray, G. R., ed. 1987. Gorda Ridge: a seafloor spreading center in the United States' Exclusive Economic Zone. New York, Springer, 311 p.

Moore, G. W., and Sharman, G. F. 1970. Summary of SCAN site 4. *In* McManus, D. A.; Burns, R. E.; et al., eds. Initial reports of the Deep Sea Drilling Project, 5. Washington, D.C., Government Printing Office, p. 761–773.

Morton, J. L., and Fox, C. G. 1994. Structural setting and interaction of volcanism and sedimentation at Escanaba Trough: geophysical results. *In* Morton, J. L.; Zierenberg, R. A.; and Reiss, C. A., eds. Geologic, hydrothermal, and biologic studies at Escanaba Trough, Gorda Ridge, offshore northern California. U.S. Geol. Surv. Bull. 2022, p. 21–43.

Morton, J. L.; Zierenberg, R. A.; and Reiss, C. A. 1994*a*. Geologic, hydrothermal, and biologic studies at Escanaba Trough: an introduction. *In* Morton, J. L.; Zierenberg, R. A.; and Reiss, C. A., eds. Geologic, hydrothermal, and biologic studies at Escanaba Trough, Gorda Ridge, offshore northern California. U.S. Geol. Surv. Bull. 2022, p. 1–18.

———. 1994*b*. Geologic, hydrothermal, and biologic studies at Escanaba Trough, Gorda Ridge, offshore northern California. U.S. Geol. Surv. Bull. 2022, 359 p.

Mulder, T., and Syvitski, J. P. M. 1995. Turbidity currents generated at mouths of rivers during exceptional discharges to the world oceans. J. Geol. 103:285–299.

Mutti, E.; Davoli, G.; Tinterri, R.; and Zavala, C. 1996. The importance of ancient fluvio-deltaic systems dominated by catastrophic flooding in tectonically active basins. Mem. Sci. Geol. 48:233–291.

Normark, W. R.; Gutmacher, C. E.; Zierenberg, R. A.; Wong, F. L.; and Rosenbauer, R. J. 1994. Sediment fill of Escanaba Trough. *In* Morton, J. L.; Zierenberg, R. A.; and Reiss, C. A., eds. Geologic, hydrothermal, and biologic studies at Escanaba Trough, Gorda Ridge, offshore northern California. U.S. Geol. Surv. Bull. 2022, p. 91–129.

Normark, W. R., and Reid, J. A. 1998. Tufts deep-sea fan: a gateway for catastrophic turbidity currents that filled Escanaba Trough, southern Gorda Ridge. EOS Trans. Am. Geophys. Union 79:F511.

Normark, W. R.; Reid, J. R.; Ross, S. L.; and Zierenberg, R. A. 1997. Tectonism and turbidites in Escanaba Trough, southern Gorda Ridge. EOS Trans. Am. Geophys. Union 78:F630.

O'Connor, J. E., and Baker, V. R. 1992. Magnitudes and implications of peak discharges from glacial Lake Missoula. Geol. Soc. Am. Bull. 104:267–279.

Ross, S. L.; Klitgord, K. D.; Reid, J. A.; and Zierenberg, R. A. 1996. New sidescan imagery of NESCA site at Escanaba Trough, southern Gorda Ridge. EOS Trans. Am. Geophys. Union 77:F316.

Scheidegger, K. F.; Kulm, L. D.; and Piper, D. J. W. 1973. Heavy mineralogy of unconsolidated sands in northeastern Pacific sediments: leg 18, Deep Sea Drilling Project. *In* Kulm, L. D.; von Huene, R.; et al., eds. Initial Reports of the Deep Sea Drilling Project, 18.

Washington, D.C., Government Printing Office, p. 877–887.
Shaw, J.; Munro-Stasiuk, M.; Sawyer, B.; Beaney, C.; Lesemann, J.; Musacchio, A.; Rains, B.; and Young, R. R. 1999. The Channeled Scabland: back to Bretz? Geology 27:605–608.
Shipboard Scientific Party. 1970. Site 35. *In* McManus, D. A.; Burns, R E.; et al., eds. Initial Reports of the Deep Sea Drilling Project, 5. Washington, D.C., Government Printing Office, p. 165–202.
———. 1973. Site 174. *In* Kulm, L. D.; von Huene, R.; et al., eds. Initial Reports of the Deep Sea Drilling Project, 18. Washington, D.C., Government Printing Office, p. 97–167.
———. 1997. Site 1020. *In* Lyle, M.; Koizumi, I.; et al., eds. Proc. Ocean Drilling Program Init. Rep. 167. College Station, Tex., p. 389–429.
———. 1998*a*. Escanaba Trough: Central Hill (Site 1038). *In* Fouquet, Y.; Zierenberg, R. A.; et al., eds. Proc. Ocean Drilling Program, Init. Rep. 169. College Station, Tex., p. 253–298.
———. 1998*b*. Escanaba Trough: Reference Site (Site 1037). *In* Fouquet, Y.; Zierenberg, R. A.; et al., eds. Proc. Ocean Drilling Program, Init. Rep. 169. College Station, Tex., p. 205–251.
———. 1998*c*. Introduction: investigation of hydrothermal circulation and genesis of massive sulfide deposits at sediment-covered spreading centers at Middle Valley and Escanaba Trough. *In* Fouquet, Y.; Zierenberg, R. A.; et al., eds. Proc. Ocean Drilling Program, Init. Rep. 169. College Station, Tex., p. 7–15.
Smith, G. A. 1993. Missoula flood dynamics and magnitudes inferred from sedimentology of slack-water deposits on the Columbia Plateau, Washington. Geol. Soc. Am. Bull. 105:77–100.
Smith, W. H. F., and Sandwell, D. T. 1997. Global sea floor topography from satellite altimetry and ship depth soundings. Science 277:1956–1962.
Snavely, P. D., Jr. 1987. Tertiary geologic framework, neotectonics, and petroleum potential of the Oregon-Washington continental margin. *In* Scholl, D. W.; Grantz, A.; and Vedder, J. G., eds. Geology and resource potential of the continental margin of western North America and adjacent ocean basins—Beaufort Sea to Baja California. Circum-Pacific Council for Energy and Mineral Resources, Earth Science Series 6: 305–335.
Southon, J. R.; Nelson, D. E.; and Vogel, J. S. 1990. A record of past ocean-atmosphere radiocarbon difference from the northeast Pacific. Paleoceanography 5: 197–206.
Spencer, P. K. 1989. A small mammal fauna from the touchet beds of Walla Walla County, Washington: support for the multiple-flood hypothesis. Northwest Sci. 63:167–174.
Steele, W. K. 1991. Paleomagnetic evidence from repeated glacial Lake Missoula floods from sediments of the Sanpoil River Valley, northeastern Washington. Quat. Res. 35:197–207.
Vallier, T. L.; Harold, P. J.; and Gerdley, W. A. 1973. Provenances and dispersal patterns of turbidite sand in Escanaba Trough, northeastern Pacific Ocean. Mar. Geol. 15:67–87.
Waitt, R. B., Jr. 1980. About forty last-glacial Lake Missoula jökulhlaups through southern Washington. J. Geol. 88:653–679.
———. 1985. Case for periodic, colossal jökulhlaups from Pleistocene glacial Lake Missoula. Geol. Soc. Am. Bull. 96:1271–1286.
Whetten, J. T.; Kelly, J. C.; and Hanson, L. G. 1969. Characteristic of Columbia River sediment and sediment transport. J. Sediment. Petrol. 39:1149–1166.
Wolf, S.; Nelson, C. H.; and Hamer, M. 1999. Turbidite pathways on Cascadia Basin and Tufts Abyssal Plain: part A, Astoria channel to Mendocino channel. U.S. Geol. Surv. Open-File Rep. 99-157, 7 p.
Zierenberg, R. A.; Morton, J. L.; Koski, R. A.; and Ross, S. L. 1994. Geologic setting of massive sulfide mineralization in Escanaba Trough. *In* Morton, J. L.; Zierenberg, R. A.; and Reiss, C. A., eds. Geologic, hydrothermal, and biologic studies at Escanaba Trough, Gorda Ridge, offshore northern California. U.S. Geol. Surv. Bull. 2022, p. 171–197.
Zuffa, G. G. 1980. Hybrid arenites: their composition and classification. J. Sediment. Petrol. 50:21–29.
———. 1985. Optical analyses of arenites: influence of methodology on compositional results. *In* Zuffa, G. G., ed. Provenance of Arenites: NATO-ASI. Dordrecht, Reidel, p. 165–189.
———. 1987. Unravelling hinterland and offshore palaeogeography from deep-water arenites. *In* Leggett, J. K., and Zuffa, G. G., eds. Marine clastic sedimentology, models and case studies. London, Graham & Trotman, p. 39–61.
Zuffa, G. G.; De Rosa, R.; and Normark, W. R. 1997. Shifting sources and transport paths for the late Quaternary Escanaba Trough sediment fill (northeast Pacific). G. Geol. 59:35–53.